FINAL REPORT

DESIGN, FABRICATION, GROUND RESONANCE AND WIND TUNNEL TEST OF A WIND-TUNNEL MODEL FOR AN EFFICIENT ALL-MOVABLE FIN DESIGN FOR AIRCRAFT

EOARD CONTRACT F61775-01-WE081

Dr M Amprikidis, Prof. O Sensburg & Prof. J.E. Cooper
School of Engineering
University of Manchester
Oxford Road
Manchester, M13 9PL, UK.

21st September 2002

REPORT DOCUMENTATION PAGE

Form Approved OMB No. 0704-0188

1. REPORT DATE ***(DD-MM-YYYY)*** 30-10-2002	**2. REPORT TYPE** Final Report	**3. DATES COVERED** *(From – To)* 19 September 2001 - 19-Sep-02

4. TITLE AND SUBTITLE

Design, Fabrication and Test of a Wind-Tunnel Model for an Efficient All-Movable Fin Design for Military Aircraft

5a. CONTRACT NUMBER F61775-01-WE081

5b. GRANT NUMBER

5c. PROGRAM ELEMENT NUMBER

6. AUTHOR(S)

Professor Jonathan E Cooper

5d. PROJECT NUMBER

5d. TASK NUMBER

5e. WORK UNIT NUMBER

7. PERFORMING ORGANIZATION NAME(S) AND ADDRESS(ES)

University of Manchester
Oxford Road
Manchester M13 9PL
United Kingdom

8. PERFORMING ORGANIZATION REPORT NUMBER

N/A

9. SPONSORING/MONITORING AGENCY NAME(S) AND ADDRESS(ES)

EOARD
PSC 802 BOX 14
FPO 09499-0014

10. SPONSOR/MONITOR'S ACRONYM(S)

11. SPONSOR/MONITOR'S REPORT NUMBER(S) SPC 01-4081

12. DISTRIBUTION/AVAILABILITY STATEMENT

Approved for public release; distribution is unlimited.

13. SUPPLEMENTARY NOTES

14. ABSTRACT

This report results from a contract tasking University of Manchester as follows: A generic all-movable vertical tail will be developed to investigate Diverging Flexible Vertical Tail Technology (DFVT). This model will be a modified version of an existing (U. of Manchester) carbon fiber composite transonic model. This model will have its boundary conditons adjusted based upon results of a previous analytical optimization study that examined weight, performance and observable benefits. A number of different parameters including: Mach number · both sub and supersonic speeds, attachment position, and variable attachment stiffnesses will also be examined experimentally in the wind tunnel at the University of Manchester, United Kingdom.

15. SUBJECT TERMS

EOARD, Structural Dynamics, Aerodynamics, Aeroelasticity, Aircraft Design

16. SECURITY CLASSIFICATION OF: a. REPORT	b. ABSTRACT	c. THIS PAGE	**17. LIMITATION OF ABSTRACT**	**18, NUMBER OF PAGES**	**19a. NAME OF RESPONSIBLE PERSON**
UNCLAS	UNCLAS	UNCLAS	UL		Wayne Donaldson
					19b. TELEPHONE NUMBER *(Include area code)* +44 (0)20 7514 4299

Standard Form 298 (Rev. 8/98)
Prescribed by ANSI Std. Z39-18

Design, Fabrication, Ground Resonance and wind tunnel test of a Model for an Efficient ALL-MOVEABLE Fin Design for Aircraft

FINAL REPORT F61775-01-WE081, Air Force, EOARD London

Michael Amprikidis, Jonathan Cooper and Otto Sensburg
Manchester School of Engineering
University of Manchester
Oxford Road, Manchester, M13 9PL, UK

SUMMARY

This report describes a 12 month project undertaken at the University of Manchester with EOARD funding during the period September 2001 – September 2002. Relevant background studies related to the design of aircraft fins prior to this project are summarized. The design, fabrication and testing of an all-moving fin wind tunnel model are described along with simulations of the aeroelastic behavior. The test results show a good agreement with the theoretical predictions and indicate that the suggested aeroelastic benefits of all-moving vertical tails are possible.

1. INTRODUCTION

In the past, conventional aircraft design practice has been to minimize elastic structural deflections in order to reduce undesirable aeroelastic phenomena. For vertical tails of high speed aircraft this has resulted in reduced stability and control effectiveness at high dynamic pressures. Consequently, adequate tail performance has required a large surface area with high aspect ratios and a stiff and heavy structure. These large surfaces are also subject to burst vortex or shock induced buffet that lead to fatigue problems. The size and structural constraints cause weight, drag, and radar-cross section penalties.

A shift has arisen during the past few years in aeroelastic design philosophy whereby these elastic deflections can be used to enhance the aeroelastic and aerodynamic performance. The technology applied is called Active Flexible Technology which is a multidisciplinary, synergistic technology that integrates aerodynamics, controls, and structures together to maximize air vehicle performance shapes for optimum performance. This was first described extensively in [1] and [5]. Large weight savings, or performance improvements, can be expected by using the advantages of flexibility. In order to satisfy the other aeroelastic constraints (flutter, divergence, vibration response, etc.) it is necessary to approach the problem in a multidisciplinary manner. If Multidisciplinary Design Optimization (MDO) is not used, then an optimal design cannot be achieved due to the conflicting demands of the different disciplines.

Work at the University of Manchester has considered the application of aeroelastic optimization technologies to the vertical tail design problem, which results in a lighter structure and potentially smaller size to reduce buffet, drag and observability. In some cases the smaller size requirement could remove the necessity for multiple surfaces.

For high speeds, the vertical tail is designed to provide a certain minimum value of the directional static stability derivative. For low speed the rudder power must be adequate to hold a sideslip of $\beta = 11.50^{o}$ at the approach speed for a cross wind landing. It also must cover the one engine out case. This low speed requirement may reduce the possibility to cut the fin span and area, commensurate with positive high speed aeroelastics.

These requirements are the same for transport and fighter airplanes. Design load cases are also equivalent and aspect ratios, taper ratios and sweep are very similar. Therefore, findings for combat aircraft are applicable to transport airplanes.

A Diverging Flexible Vertical Tail (DFVT) could be very useful for short fuselage versions if the static stability is a problem reducing the necessary span and weight. The reason why it is called 'diverging' is that a surface design with greater efficiency than 1.0 must diverge at some speed. Our aim must be that the divergence does not occur in the required speed range of the air vehicle.

If the low speed requirement is the design case, then an all moveable vertical tail could be the solution. An all moveable vertical tail is not a new invention. It was utilized on the very successful VSR71 Blackbird and on the VF117 stealth fighter. Also a British prototype aircraft of the 1960's, the TSR2, had an all-moveable vertical tail. It was also considered seriously on the European fighter aircraft, EFA. All-moveable vertical tails were also discussed in [2]. In the context of the DFVT it has several advantages:

- The rear yaw attachment can be moved far backward on the fin, because there is no rudder.
- It can also be utilized for the low speed regime (engine out or side wind requirement) where there is no aeroelastic effect, because the whole surface is rotated.

This report briefly describes some of the previous work at the University of Manchester relating to the optimal design of aircraft vertical tails with multiple and single attachments. The work reported here describes the design, fabrication and test of an all-moving vertical tail wind tunnel model. Results from the tests are compared with those from an analytical study in order to determine experimentally whether the aeroelastic benefits of all-moveable vertical tails seen in analysis actually occur in practice.

2. PREVIOUS WORK

There have been two previous studies at the University of Manchester related to this project funded by the EOARD.

2.1 Aeroelastic Tailoring of a Vertical Tail With Multiple Attachments

The first project considered the aeroelastic tailoring of a vertical tail and showed that it is possible to achieve a directional stability derivative that is thirty percent higher than that of a rigid tail. Using this design feature the span and weight can be reduced accordingly.

A generic aircraft design was selected, and the vertical tail was designed (at the conceptual design level) with conventional and active flexible technologies. The weight, performance, and observables benefits of the DFVT were then determined relative to the conventional design. Figure 1 shows the comparison of a fighter vertical tail with the vertical tail of a future large transport aircraft. Because of the low aspect ratio of the chosen vertical tail design, AR=1.2, this is an ideal candidate for applying aeroelastic tailoring for a carbon fiber composite structure. As can be seen in figure 2, the higher the aspect ratio is, the higher are the weight penalties to meet the performance goals.

A Finite Element Model (FEM) model was available which was used in the Dasa Lagrange optimization code [3]. This model was modified to serve for the USAF-ASTROS optimization code. This FEM could be very useful for future work in this area as a benchmark.

The weight of the fin was selected as the objective function. The response constraints were derived from the simultaneous analysis of the structure in three areas: a) static strength, b) static aeroelastic response and c) dynamic aeroelasticity - flutter. The variables to be adjusted were the thickness and directional properties of the fiber reinforced composite skins.

The optimization problem was to find the optimal variable vector that corresponds to the minimum weight of the structure without violating any of the response constraints and pre-defined ranges.

- Strength or strain allowables must not be exceeded. Five load cases were used in this case.
- Static aeroelastic efficiencies for the vertical tail and the rudder were required. These are defined as flexible coefficients divided by the rigid coefficients.
- Flutter or divergence speed requirements, 530m/sec, Ma 1.2 for this case. For the transport aircraft it is reduced to 400 m/sec, Ma 0.9, which gives a relief, because static aeroleastic efficiency and flutter speed are conflicting targets.

In order to become familiar with the Dasa finite element model of the fin and rudder several NASTRAN and ASTROS analyses were performed, and the results were compared with existing Dasa data. Correlation was found to be excellent. After that exercise the Dasa model was changed. To allow different attachment conditions the general stiffness element, GENEL, giving the effect of the fuselage stiffness, was removed and replaced with single attachment springs. These springs were tuned so that the model would give the original Dasa result. ASTROS and NASTRAN results are identical, because the ASTROS-code uses the finite element description of NASTRAN. The results of this comparison can be found in Table 1.

Several computer runs were performed with

- Strength Constraints
- Flutter speed 530/m/sec at Ma 1.2/S.L.
- Aeroelastic Efficiency

trying to match the Dasa results for a fin efficiency of 0.814 at Ma 1.8, 102 kPa. The rudder efficiency was fallout at 0.3799. The ASTROS code reduced the weight for this configuration to 81.1 kg. The weight of the initial design was 99.4 kg. When all the constraints were fulfilled, the weight was 95.1 kg for a fin efficiency of 0.814.

Higher fin efficiencies were requested, and the weights for these designs are plotted in Fig. 4. While 0.9 can be reached with very little extra weight, higher efficiencies need excessive weight penalties. When the rudder efficiency was treated as fallout, then the weight reduces considerably, and an efficiency of 1.0 can be reached when flutter is fallout too. The fallouts are quite reasonable and sufficient for a feasible design. From Fig. 4 it can be seen that a fin efficiency of 1.0 can only be achieved with infinite weight.

The picture changes completely when Ma 0.9 subsonic air forces are used (Fig. 5). Now efficiencies higher than 1.0 are reached. As can be seen, with very little additional weight, 1.3 can be reached for a high pressure of 102 kPa, which is not possible for air. The highest q is 57 kPa for Ma 0.9, i.e. sea level in air. This trend is also verified in Fig.6 which clearly shows that the wash-in angle increases for higher efficiencies, which simulates basically a forward swept fin behavior (diverging!).

In order to understand the elastic behavior of the fin, an equivalent beam is assumed which contains the stiffness of the fin. This beam would be located at the elastic axis, which is a spanwise line through the shear centers of each cross section. The shear center of each cross section is computed by establishing the point in the plane of the section at which a shear force can be applied without twisting the section or where a twisting moment can be applied to the section without producing a deflection at the shear center. An effective elastic axis was defined by using the deflection of two points fore and aft on the chord, where a moment was applied at the tip, assuming small angles and that the deflection varies linearly along the chord. Fig. 7 shows the elastic axis location. From this figure one can assess why it is impossible to get a wash-in effect (diverging) for the supersonic Ma 1.8 case. The center of pressure – at 30% span and 50% chord – just reduces any initial angle of attack of the fin, and therefore the best fin efficiency which can be reached with aeroelastic tailoring is 1.0, which is the rigid behavior and needs a lot of structural weight. At the subsonic case, Ma 0.9, there exists some possibilities for wash-in, because the aeroelastic tailoring also shifts the so called elastic axis. This behavior is shown in Fig. 5 and also in Fig. 8 for an optimized case of Ma 0.9, 102 kPa and fin efficiency of 1.3.

This behavior changes drastically when the fin attachments are shifted back. The x-position for the forward attachment was shifted back from x = 450mm to x = 950 mm. The x-position for the rear attachment was shifted from x = 1750 mm to x =2300 mm. The new positions can be seen in Fig. 9. Now the centers of pressure are forward of the elastic axis, and wash-in behavior can be expected for both the subsonic and the supersonic cases (Fig. 9). For Ma 0.9, 57 kPa a fin efficiency of 1.3 can be reached with practically no weight increase. Also the rudder efficiency increases from 0.5 to 0.7. This can be seen in Figure 10. For the supersonic case Ma 1.8, 102kPa the behavior is similar (Fig. 11), and 1.3 can also be reached with an optimized laminate. The rudder efficiency is now reduced to 0.5. The flutter speed is 530m/sec. As an item of interest an analysis was performed (no optimization) to find the fin and rudder efficiency at Ma

0.9, 57kPa for the laminate of Ma 1.8, 102 kPa. This shows a fin efficiency of 1.3 and a rudder efficiency of 0.8.

The conclusions of this initial piece of work showed that the use of MDO methods could improve significantly the design of composite vertical tails. Possible benefits could be:

- The reduced tail size reduces the C_{D0} drag.
- The reduced span and area reduces the exposure to upstream induced burst vortex and separated flow unsteady pressure fields which increases tail buffet fatigue life. The increase in life reduces repair and replacement life cycle costs.
- The reduced planform size reduces observable signatures to increase stealth mission capability and reduce detectability.
- Because of the possible size reduction one vertical tail should be sufficient even for Navy airplanes.
- With proper multidisciplinary optimization a carbon fiber vertical tail can be made 30% more efficient that a rigid surface at the same weight.
- If the low speed requirement is not relevant, the area of the vertical tail can be reduced by 30% together with the structural weight.

Of greater interest to this work was the further conclusion that changing the attachment position had a very large effect on the aeroelastic behaviour, in particular, moving the attachments rearwards gave beneficial aeroelastic effects, as seen in figure 12. Very preliminary investigations had shown that these advantages could be greater if only a single attachment were used.

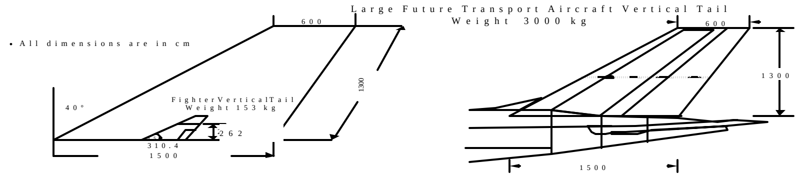

Fig 1 Comparison of a fighter vertical tail with the vertical tail of a future large transport aircraft

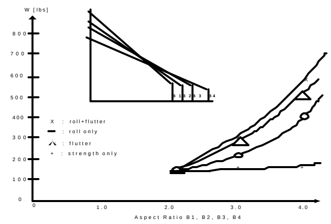

Fig 2 Structural weight for various constraints vs aspect ratio

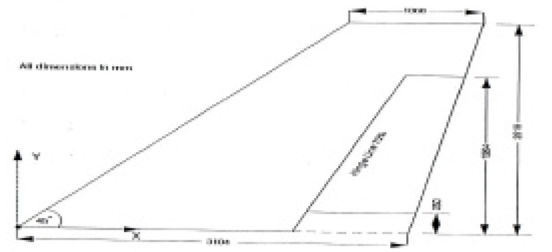

Fig 3 Fin Geometry

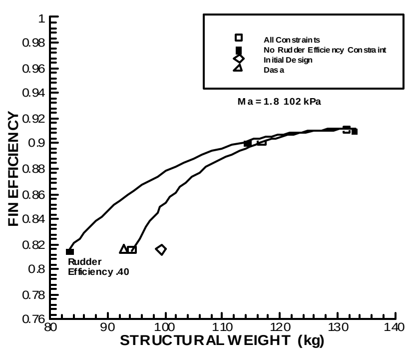

Fig 4 Fin efficiency vs structural weight
Ma 1.8 102kPa

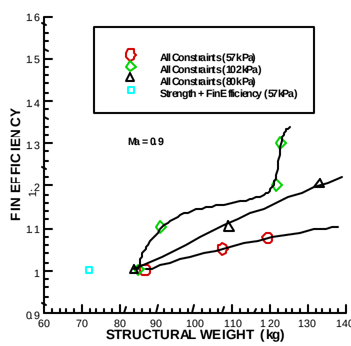

Fig 5 Fin efficiency vs structural weight
Ma 0.9

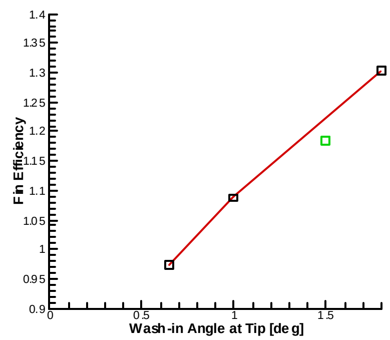

Fig 6 Fin efficiency vs wash-in angle
at the tip

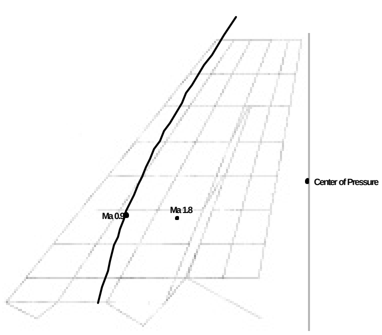

Fig 7 Elastic axis location (original attachments
and DASA skin thicknesses)

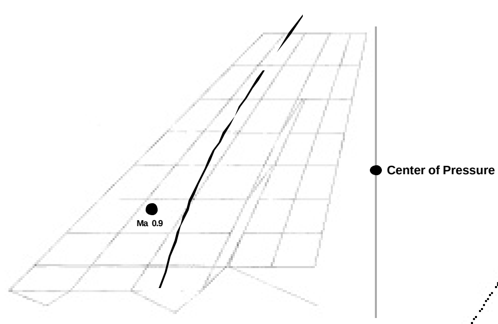

Fig 8 Elastic axis location
for Ma 0.9 102kPa
fin efficiency 1.3

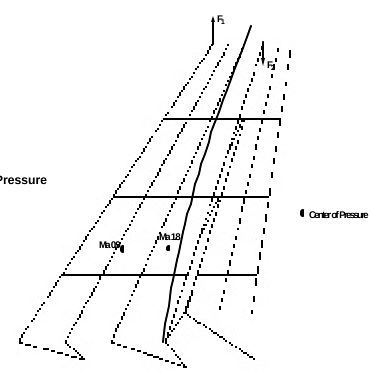

Fig 9 Elastic axis location
(rear attachments)

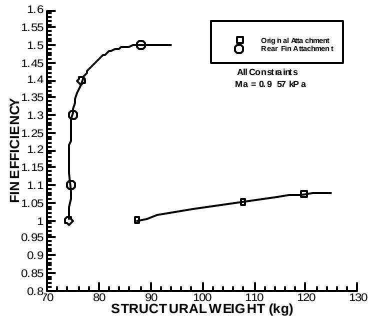

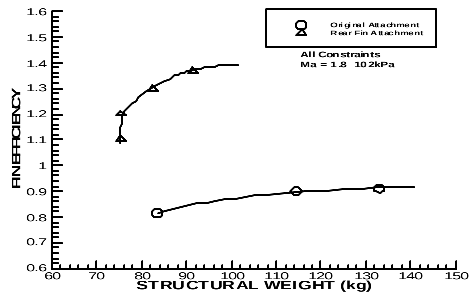

Fig 10 Fin efficiency vs structural weight
Ma 0.0 57 kPa

Figure 11 Fin efficiency vs structural weight
Ma 1.8 102 kPa

	Initial Design ASTROS	Initial Design DASA	With Single Springs	Optimum Design	
				ASTROS	DASA
Weight [kg]					
Structure	99.4	99.4	99.4	94.3	92.9
Non Structure	53.6	53.6	53.6	53.6	53.6
Total	153.0	153.0	153.0	147.9	146.5
Deflections [mm]					
Load Case 1	304	291			
Load Case 2	384	367			
Load Case 3	148	154			
Load Case 4	220	231			
Load Case 5	146	159			
Frequencies [Hz]					
f_1	9.1	8.9	9.0	8.89	9.2
f_2	30.5	29.8	30.0	28.84 (f+a)	30.2 (f+a)
f_3	32.5(fore+aft)	31.2 (f+a)	43.9 (f+a)	41.03	30.6
f_4	41.4	40.0	41.6	42.39	41.08
f_5	55.7	54.9	57.6	59.36	58.31
Ma 1.2 S.L.					
Flutter Frequency – f_f[Hz}	20.2	21.2	20.0		
Speed – v_f [m/s]	493.4	495.0	534.0	530.0	530.0
Ma 1.8 102kPa – Aeroelastics					
Fin		0.753	0.740	0.814	0.814
Rudder		0.441	0.423	0.500	0.500
Aeroelastic Deflections [mm]					
Fin 1^0	65.34	53.7			
Rudder 1^0	8.88	8.29			

Table 1 Comparison of DASA and ASTROS Model Results

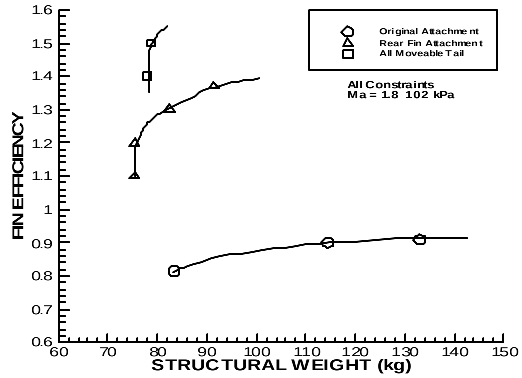

Figure 12 Fin efficiency vs structural weight for Ma 1.8 102 kPa

2.2 Analytical Investigation of the Aeroelastic Behavior of An All-Moving Vertical Tail

In the second piece of previous work, the Lagrange Multi-Disciplinary Design Optimisation (MDO) code was used to undertake a preliminary study into design aspects of a generic all-movable aircraft fin. It was shown how the control effectiveness at high speeds could be increased through variation of the attachment position and stiffness, whilst still meeting strength and aeroelastic stability constraints.

Initial studies indicated that the prime influence on the aeroelastic behaviour of the all-moveable fin would be the stiffness and position of the attachment. Consequently, the fin structure was kept the same for all cases (figure 13). The effectiveness for various attachments and Mach numbers was calculated. Also, the flutter speed for the different attachments was also determined. Figure 14 shows how the attachment was modelled. The torsional stiffness about the y axis has the greatest effect on the aeroelastic performance and this was varied throughout the investigation through adjustment of the corresponding springs.

Of key interest was the ability to improve the effectiveness of the fin. Figures 15 show the changes in the effectiveness for different attachment stiffness and flight conditions. Once the attachment is moved far enough aft, it is possible to improve upon an effectiveness of unity. This can be achieved for all of the considered Mach numbers if the stiffness is reduced sufficiently. The ability to improve upon the rigid effectiveness is essentially due to the positioning of the flexural axis relative to the aerodynamic centre.

Figures 16 shows a similar behaviour, except this time for varying attachment position. The problem with these findings of course is that we have only been considering a single parameter. When the flutter speed is considered as well, as shown in Figure 17, it can be seen that if the stiffness is reduced then, obviously, the flutter speed is reduced as well.

In conclusion, the work showed that there is a trade off between the best parameters required to achieve a good effectiveness and the flutter speed. To develop this approach further, the design will need to consider whether it is for a civil or military application. It is feasible in the latter case that a variable actuator stiffness may be required, for low and high speed conditions.

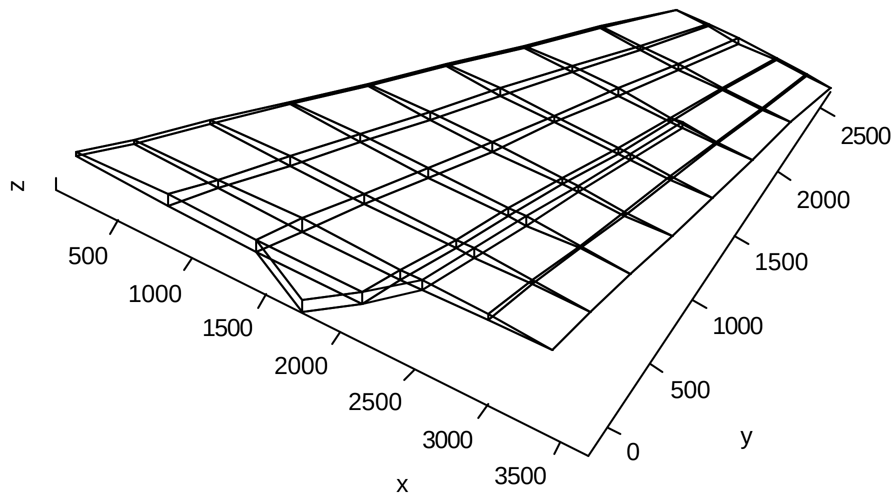

Figure 13. All-Moveable Fin

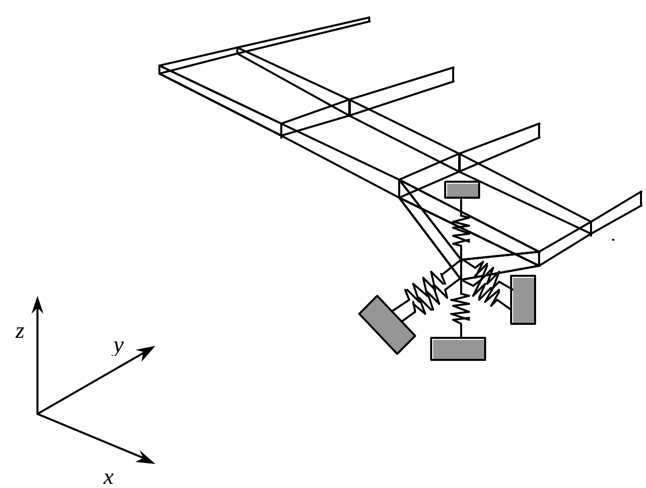

Figure 14. Modelling of Attachment

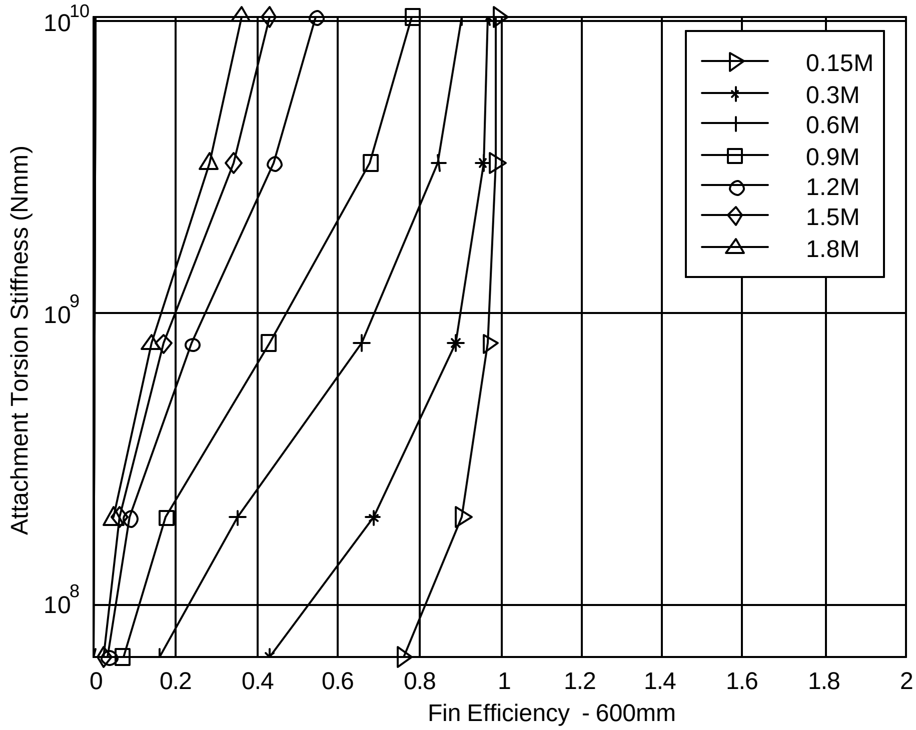

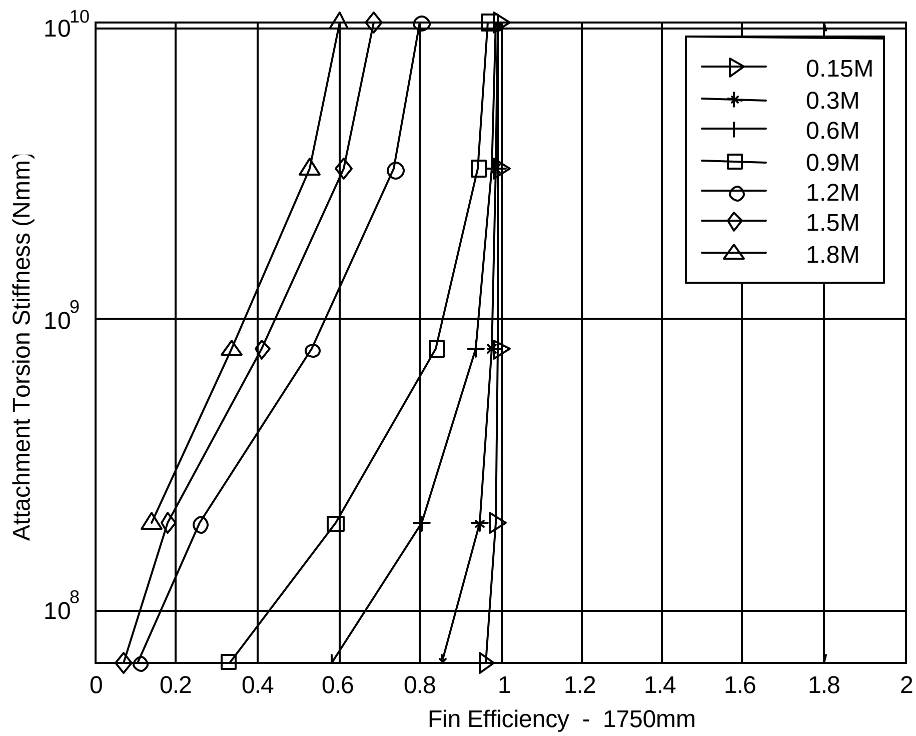

Figures 15a,15b. Fin Efficiencies Vs. Attachment Stiffnesses. 600mm and 1750mm Attachment

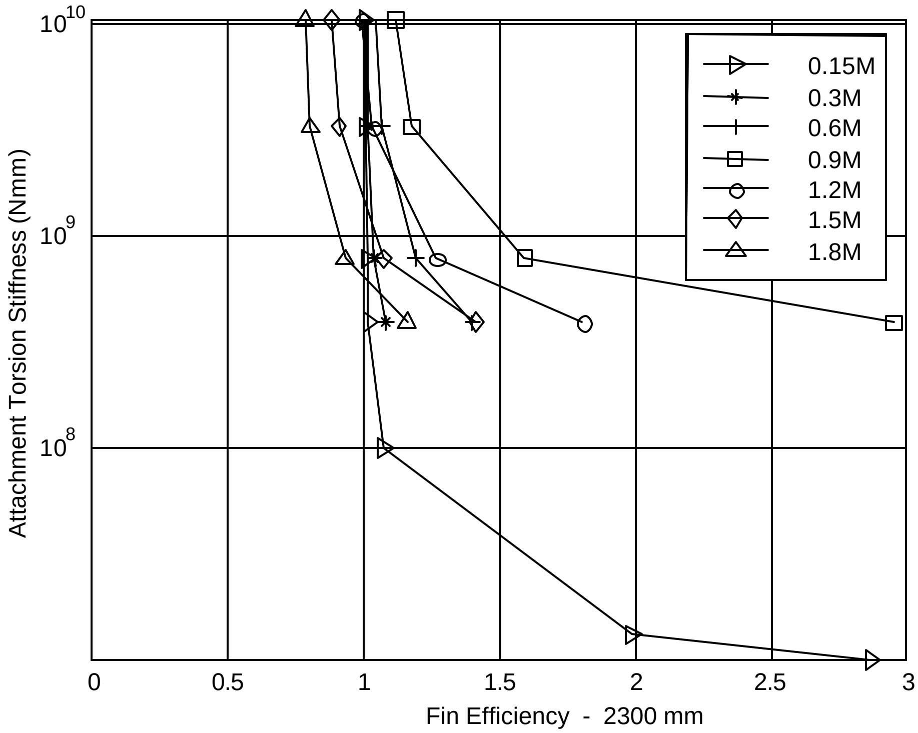

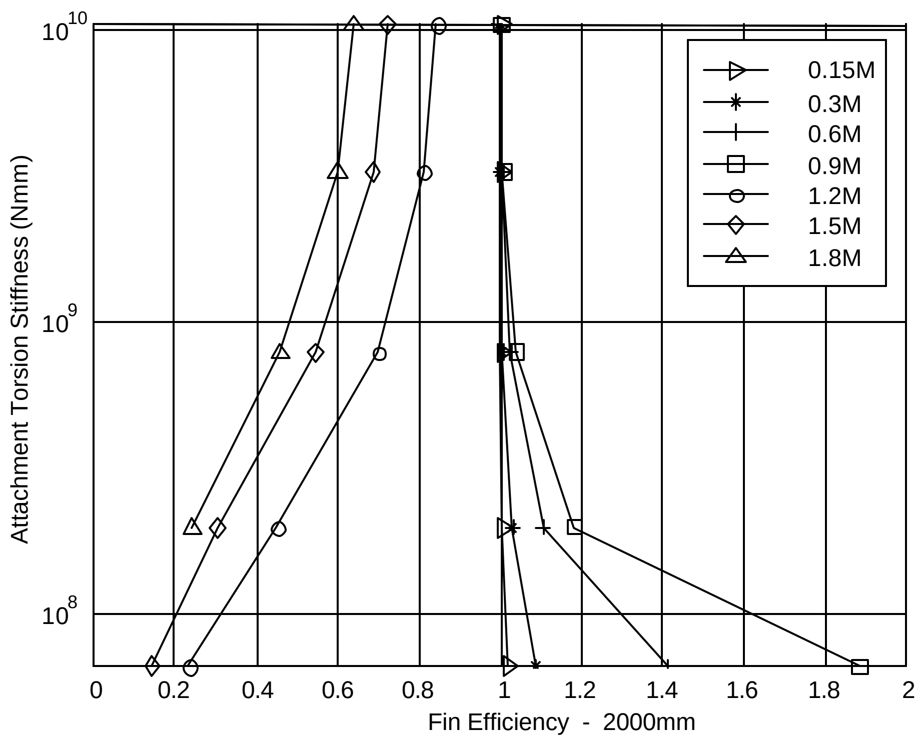

Figures 15c,15d. Fin Efficiencies Vs. Attachment Stiffnesses. 2000mm and 2300mm Attachment

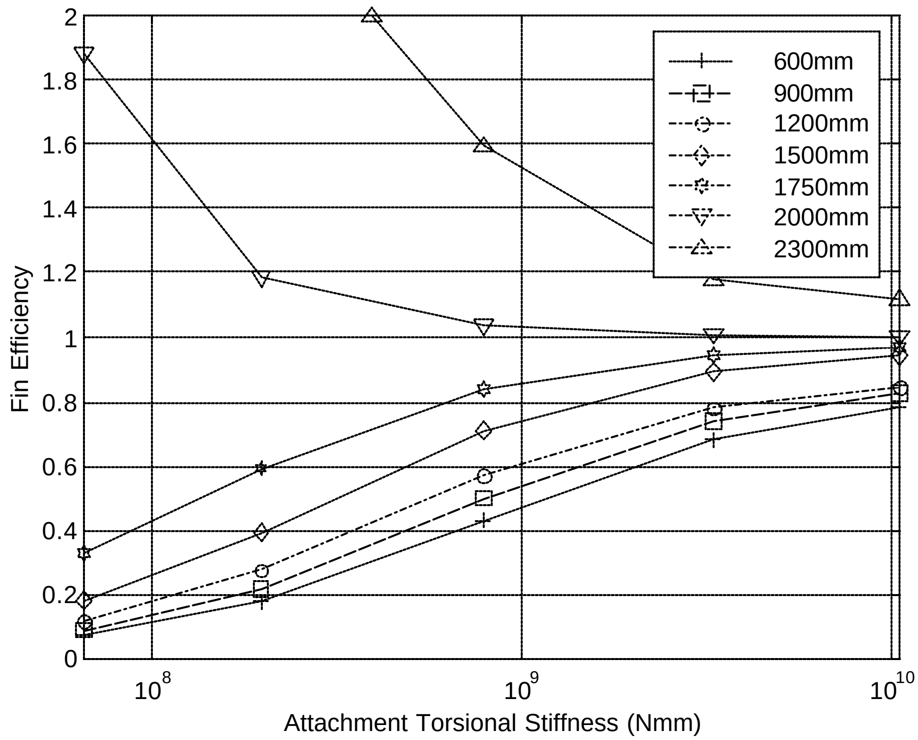

Figure 16a. Fin Efficiency VS Torsional Stiffness at 0.9 Ma

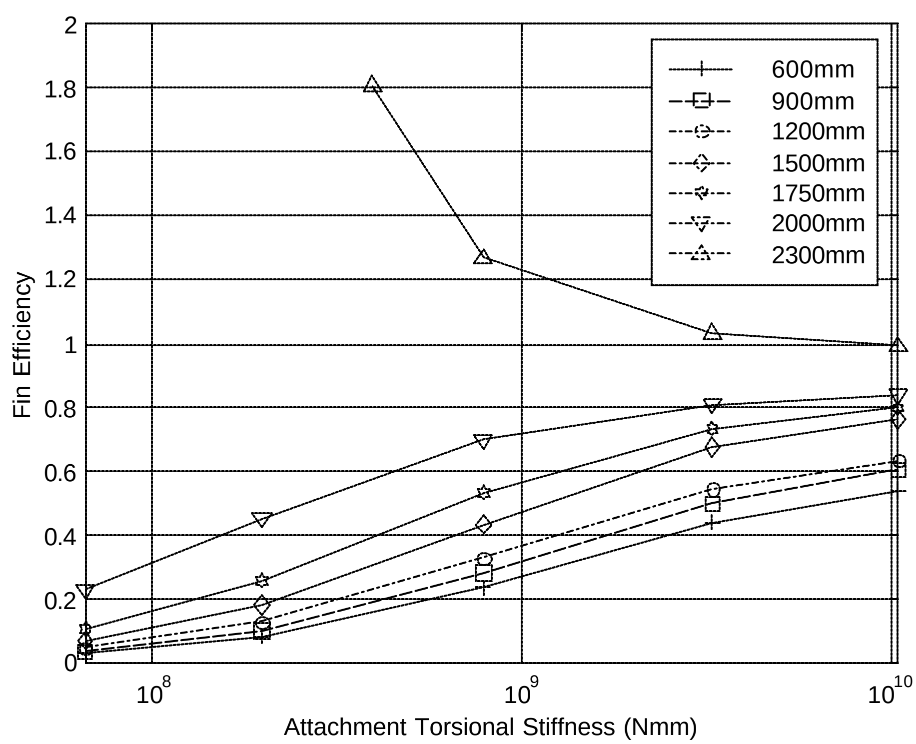

Figure 16b. Fin Efficiency VS Torsional Stiffness at 1.2 Ma

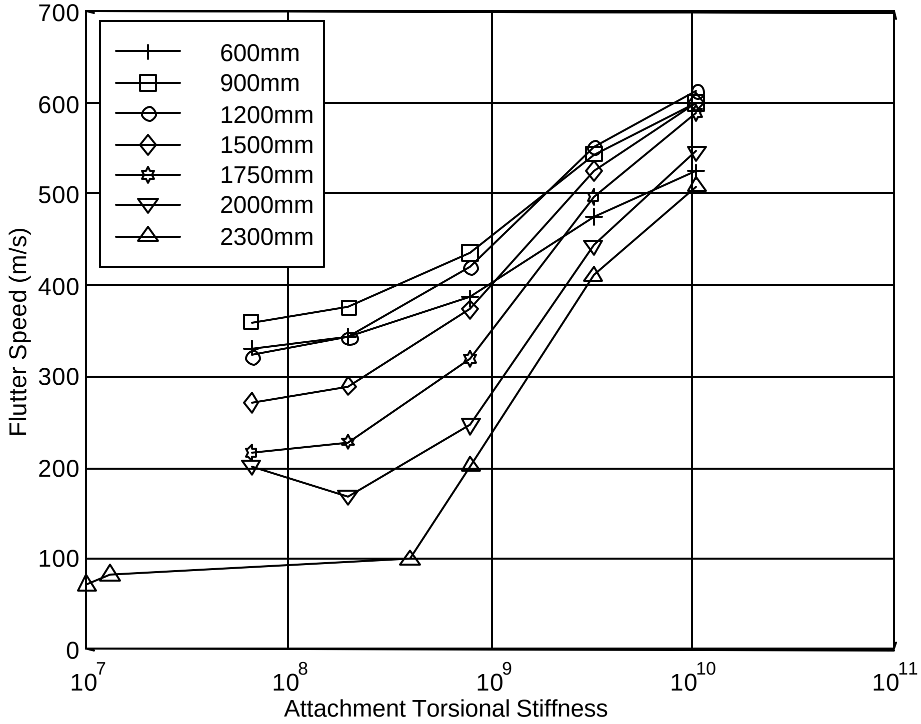

Figure 17. Variation of Flutter Speed For Different Attachments

3. All-Moving Vertical Tail Model Design, Build and Test

The objective of this investigation was to design, construct and test an all-movable fin wind tunnel model in order to establish whether the aeroelastic behaviour predicted by analysis could be replicated in test. A numerical simulation study investigated the effect of moving the attachment position and stiffness for a scaled model of the previous work described above. These results were used to define the spring stiffnesses that were needed for the actual wind tunnel test model. The attachment design and construction of the model is described along with the tests performed and the comparison with analytical predictions.

3.1 Theoretical Analysis

The simulation model used was an all moveable fin with a low aspect ratio (AR=1.2) constructed with multi-layered Carbon Fibre and Quasi Isotropic Graphite Fibre composites, as such a wind tunnel model was available for use. Figure 18 shows the finite element mesh that was used. The Lagrange MDO code was used to determine the Fin Efficiency at various speeds for different attachment positions and stiffnesses, and a typical set of results are also shown in figure 18. The speeds that the fin was analysed varied from Mach 0.1 to 1.8, and the attachment positions ranged from 120mm (forward) to 460mm (backward). The results agreed with the previous study in that it was found that it is possible to improve the fin efficiency when the fin attachment was shifted back, although there is a consequent reduction in the flutter speed.

These results enabled the design of the adjustable attachment to be made, in particular the stiffnesses of the springs that needed to be used could be defined.

3.2 Design and Construction of an All-Movable Vertical Tail

An existing wind-tunnel fin model was used, but an attachment needed to be designed so that the characteristics of an all-moving fin could be investigated and compared with the simulated studies. Figure 19 shows a schematic of the set-up. Essentially, the existing model sat upon a new base with a single attachment point whose position could be adjusted. Movement was constrained to only allow torsion about the vertical axis. There was very little extra friction in this motion as the attachment incorporated a number of bearings. The single attachment was fixed to four linear springs arranged beneath the floor of the wind tunnel. Through changes in the springs, it was possible to modify the effective torsional stiffness of the fin.

As well as investigating the behaviour of an all-moving vertical tail, it was felt necessary to reproduce at wind tunnel speeds the full scale aircraft fin of the previous studies. Hence, the velocity scale is 1.0 and the model has to be geometrically scaled factors are shown in table 2

Dimension	Scaling factor	Units
Length	0.2	Mm
Stiffness	0.2	N/mm
Torsional Stiffness	0.2^{-3}	Nmm/rad
Frequency	5.0	Hz
Mass	0.2^{3}	Kilos
Velocity	1.0	m/s

Table 2. Scale factors for wind tunnel model

Reference to figure 18 shows how the torsional spring stiffness was derived. At 0.09M, which corresponds to 30m/s at sea level, a spring was selected which produce an efficiency of 2.0 at 3.75×10^6 Nmm/rad for the most rearward attachment position of 2300mm. Assuming that we get correlation at this point with model in the wind tunnel then all the curves up to 1.8 M are confirmed with the reservations about compressibility effects, which are valid for all subsonic wind tunnel tests. The range of springs used is shown in table 3.

N/mm AC	N/mm Model	Nmm/rad AC	Nmm/rad Model
321.50	0.187	33750	33750
428.66	0.250	45000	45000
857.33	0.500	90000	90000
1714.6	1.000	180000	180000

Table 3. Linear springs used for the wind tunnel tests

The torsional stiffness of the model was calculated with an arm of 600mm whereas the arm for the aircraft is 162mm.

Figures 20-25 show various aspects of the experimental set-up, in particular the spring attachments, the variable position attachment, and also the laser measurement device. The wind tunnel used for this study in shown in figure 26, with figure 27 showing the fin inside the wind tunnel. Two different attachment positions are shown in figure 28.

Although this study was primarily concerned with the static aeroelastic behaviour, it was felt necessary to monitor both static and dynamic displacements using displacement probes. Two were used, one measuring the displacement of the spring attachment device below the tunnel floor. The second device measured the deflection of a point on the fin itself, this would pick up any motion of the fin apart from the rigid body torsional motion. No significant differences in these measurements were ever measured, due to the large stiffness of the fin compared to the attachment stiffness, and so it was a valid assumption to make that the fin was essentially rigid.

3.3 Experimental Test and Analysis

A number of initial ground resonance tests were performed on the fin structure in order to examine the behaviour of the spring attachments at a range of different attachment positions. Figure 29 shows a typical displacement response following an initial step input. A single degree of freedom motion results (as expected) and it was found that there was a good correlation between the predicted spring stiffness and the measured effective torsional stiffness.

The airflow was then turned on and the above process repeated for a range of different tunnel speeds. Figure 30 shows a sample impulse response at 20 m/s. It can be seen that the same single degree of freedom motion dominates the response, although the damping is now much greater. There is also now a certain amount of noise on the data.

A ground resonance test was performed in the wind tunnel at two attachment positions and the rigid body mode yaw frequency is shown in table 4 for an attachment stiffness of 180000 Nmm/rad.

Attachment position	120mm	460mm
Frequency	4.74 Hz	5.89 Hz

Table 4. Yaw Frequency

The elastic modes of the fin are several octaves above this mode and therefore do not play a role in the model elastic behavior. These results agreed with predictions once the inertia of the additional structure had been added. For the scaled springs used, it was determined that the divergence speed was about 40m/s (fig 31). It was therefore of no use to go to the bigger and faster Goldstein Wind Tunnel Research facility because the range of the university Wind Tunnel used was sufficient. A far more comprehensive set of tests than originally anticipated in the proposal was consequently performed in the low speed tunnel.

3.4 Wind Tunnel Test Procedure and Results

The wind tunnel test procedure consisted of setting the fin at some pre-determined angle at zero wind speed, then increasing the tunnel speed, and then measuring the resulting twist using the laser device. The efficiency was then calculated as

$$\frac{C_{Lb}\,elastic}{C_{Lb}\,rigid} = \frac{\text{YAW ANGLE elastic}}{\text{YAW ANGLE rigid}}$$

A wide of different parameters were considered, however, for the purposes of this report we shall concentrate on those described in table5.

<table>
<tr><td>7 Attachment positions</td><td>120mm</td><td>180mm</td><td>240mm</td><td>300mm</td><td>350mm</td><td>420mm</td><td>460mm</td></tr>
<tr><td>4 spring stiffnesses</td><td>1800000</td><td>90000</td><td colspan="2">45000</td><td>33750</td><td colspan="2">Nmm/rad</td></tr>
<tr><td>4 speed settings</td><td>0</td><td>10</td><td colspan="2">20</td><td>30</td><td colspan="2">M/s</td></tr>
<tr><td>Presetting of the fin</td><td colspan="3">2</td><td colspan="4">Degrees</td></tr>
</table>

Table 5. wind tunnel parameters.

The total yaw angle is plotted in figure 32 for various attachment positions, a stiffness of 33750 N/mm and a speed of 30 m/s. It is interesting to watch how the angle increases going to the rear and how it decreases going to the front attachment.

Figures 33 through to 40 show Fin efficiencies Vs Attachment Position for various stiffnesses. The lowest spring of figure 41 results in the highest efficiency of 2.05 and largest load alleviation of 0.4 for 30 m/s. comparisons of theoretical and experimental results are plotted in figures 10 to 14 for various stiffnesses and speeds. Figure 42 presents a comparison between test and theory for the highest speed at the two extreme positions. Correlation between analysis and test is good and is even closer for the lowest tested stiffness.

Differences between the analytical and simulated results were due to the level of vibration response of the model, particularly at the higher speeds that required the results to be avergaed over time. This was thought to be due to separated flows around the base of the fin and which may have deteriorated the accuracy of the test data. It should also be mentioned that because of the possibility to vary attachment position, the scaled wind tunnel model had inertia that was more than two times greater than that of the aircraft fin at the most rearward position. Therefore all dynamic wind tunnel test data cannot be used directly for comparison with the full scale analytical results.

4. CONCLUSIONS

A scaled all-moving vertical tail wind tunnel model has been designed, fabricated and tested. It was designed so that it was possible to vary the attachment stiffness and position. The static aeroelastic behaviour, in particular the effectiveness, was measured for a range of different tunnel speeds and attachment stiffness and position. These tests verified the findings of previous analytical studies in that it is possible to increase the effectiveness by moving the attachment backwards and by reducing the stiffness, however, this also reduces the flutter and divergence speeds.

5. FUTURE WORK

The concept of all-moving vertical tails should be pursued:

1. Through application to full size aircraft tails
2. Through the investigation of the feasibility of implementing an attachment with torsional stiffness that can be varied in-flight.

6. REFERENCES

[1] Shirk, M. H., Hertz, T. J., and Weisshaar, T. A., A Survey of Aeroelastic Tailoring Theory, Practice, Promise ,AIAA Paper AIAA-84-0982-CP, 25th Structures, Structural Dynamics and Materials Conference, Palm Springs, California, 1984

[2] Schweiger, D. and Krammer, J., Active Aeroelastic Aircraft and its Impact on Structure and Flight Control System Design, AVT Panel Meeting Proceedings, Ottawa, Canada, Fall 1999

[3] Schneider, G., Krammer, J. & Hornlein, H.R.E.M., First Approach to an Integrated Fin Design, AGARD Report 784, Integrated Design Analysis & Optimization of Aircraft Structures

[4] Neill, D.J., Herendeen, D.L., Venkayya, V.B., ASTROS Theoretical Manual, USAF WL-TR-95-3006

[5] Pendleton, E., Bessette, D., Field, P., Miller, G., and Griffin, K., The Active Aeroelastic Wing Flight Research Program, 39th AIAA/ASME/ASCE/AHS/ASC Structures , Structural Dynamics, and Materials Conference, April 1998

[6] Bowman, K.B., Grandhi, R.V., and Eastep, F.E., Structural Optimization of Lifting Surfaces with Divergence and Control Reversal Constraints, Structural Optimization 1, pgs 153-161, Springer-Verlag 1989

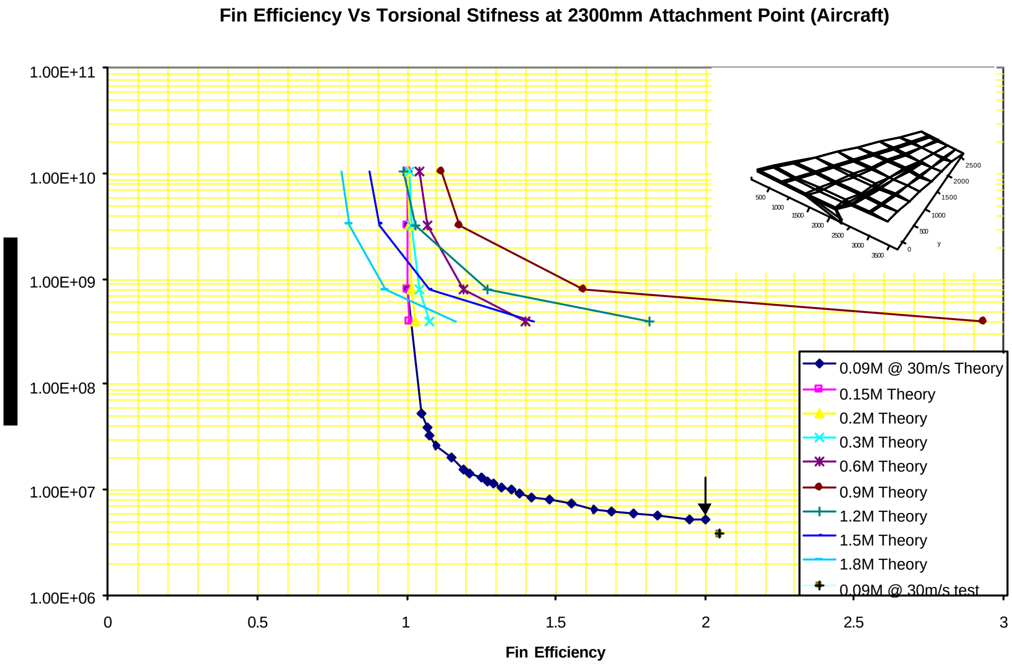

Figure18. Selection of springs for wind tunnel test

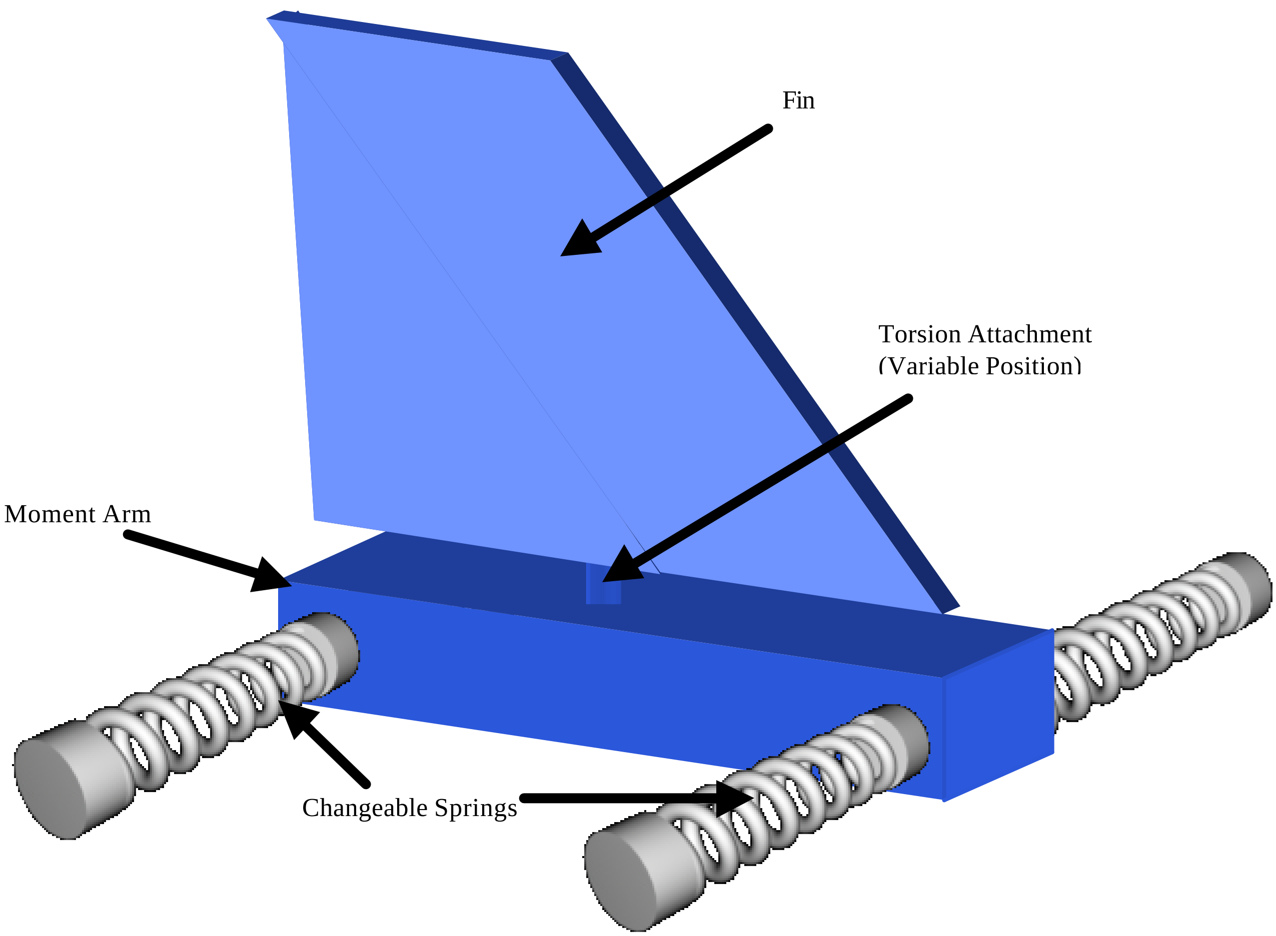

Figure 19. Schematic of the Experimental Fin Wind Tunnel Model

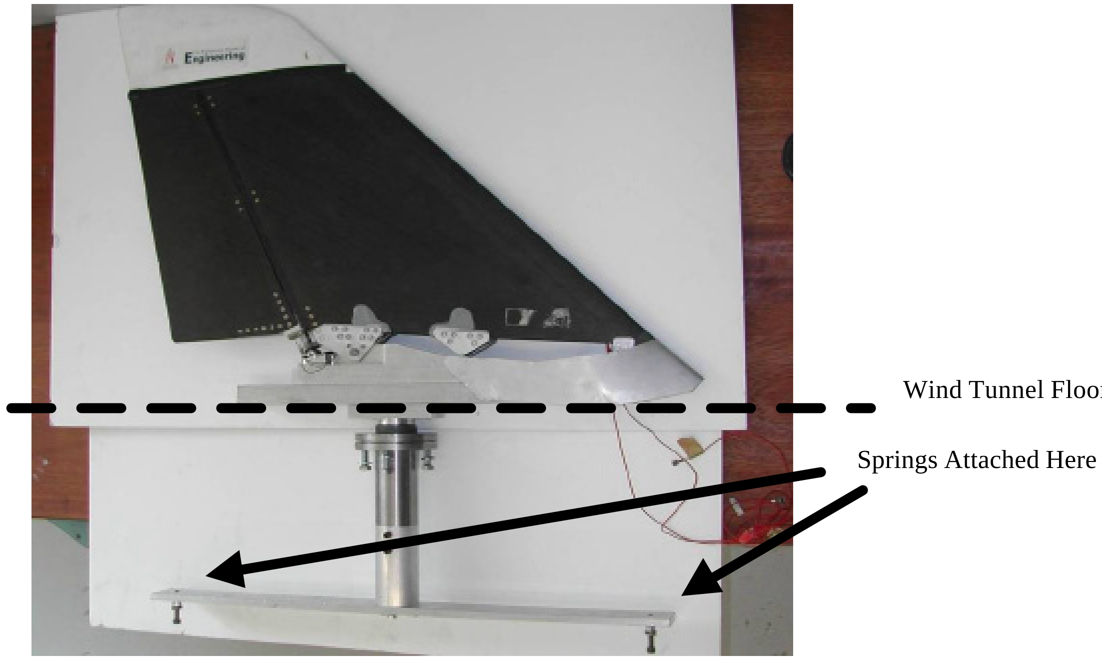

Figure 20. Fin Experimental Set-up With Arm for Spring Attachments

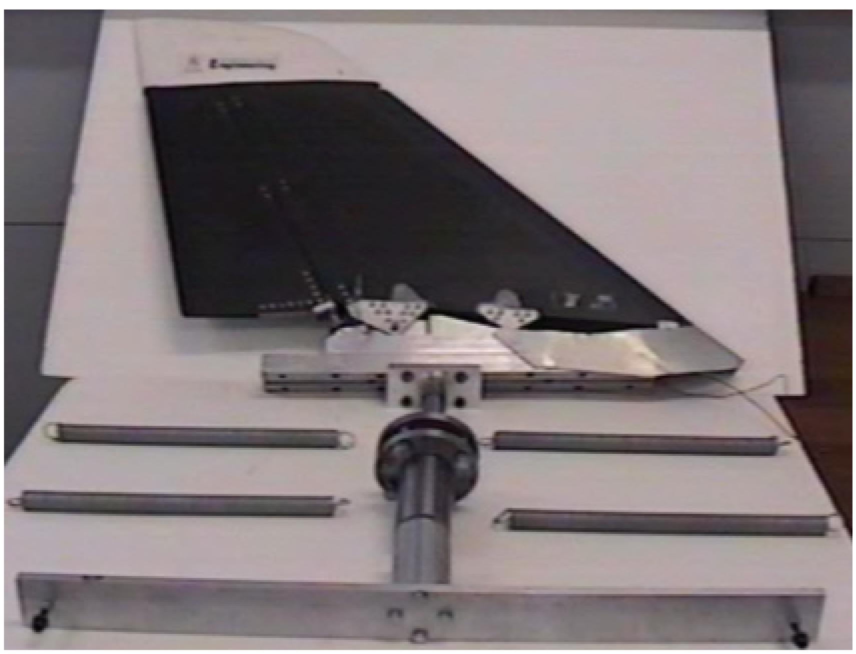

Figure 21. Fin Attachments and Springs.

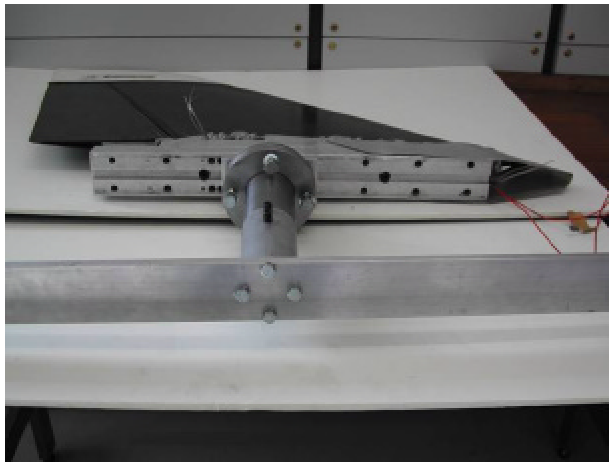

Figure 22. Close Up of Variable Position Attachment

Figure 23. Different Stiffness Springs Used in the Experiments

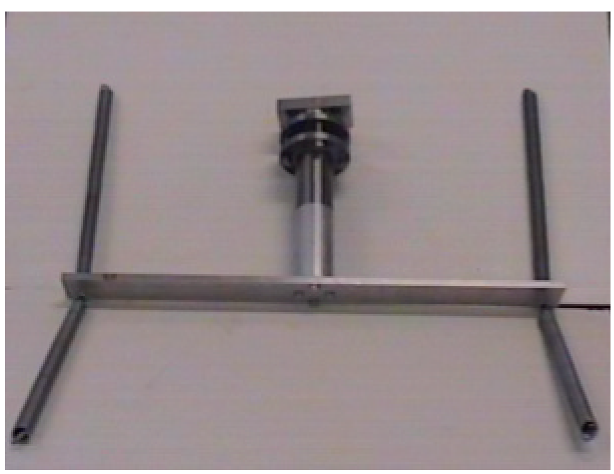

Figure 24. Springs Attached to Moment Arm

Figure 25.   Laser Displacement Probe.

Figure 26. Wind Tunnel Facility

Figure 27. All-Moving Vertical Tail in the Wind Tunnel

Figure 28. Wind tunnel and Fwd / Rear Attachment positions of the model

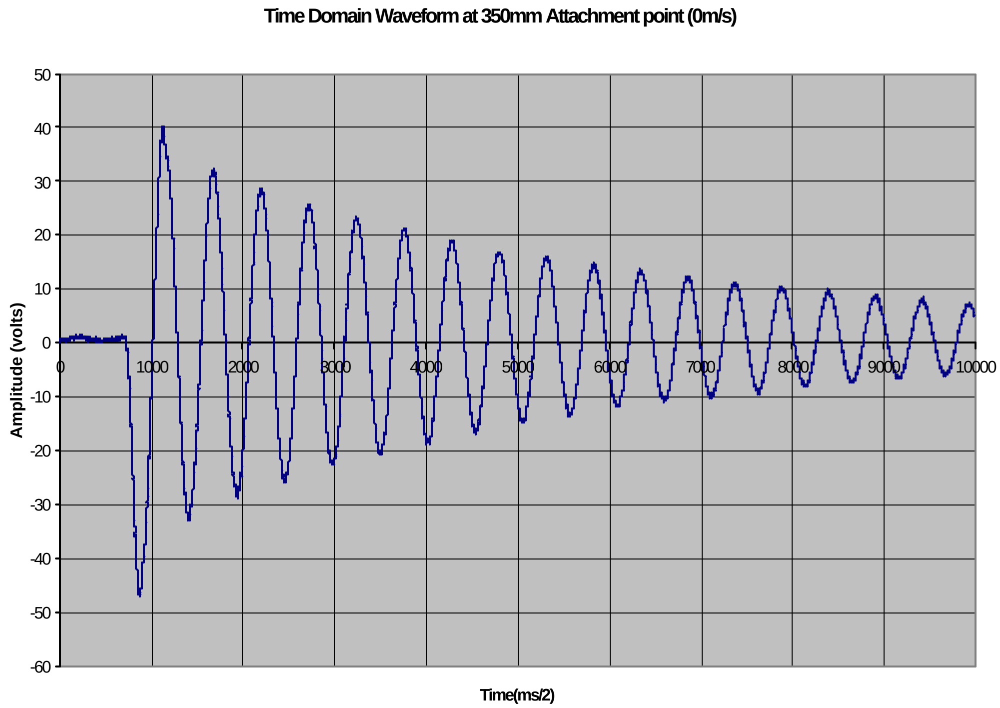

Figure 29. Impulse Response at Zero Speed.

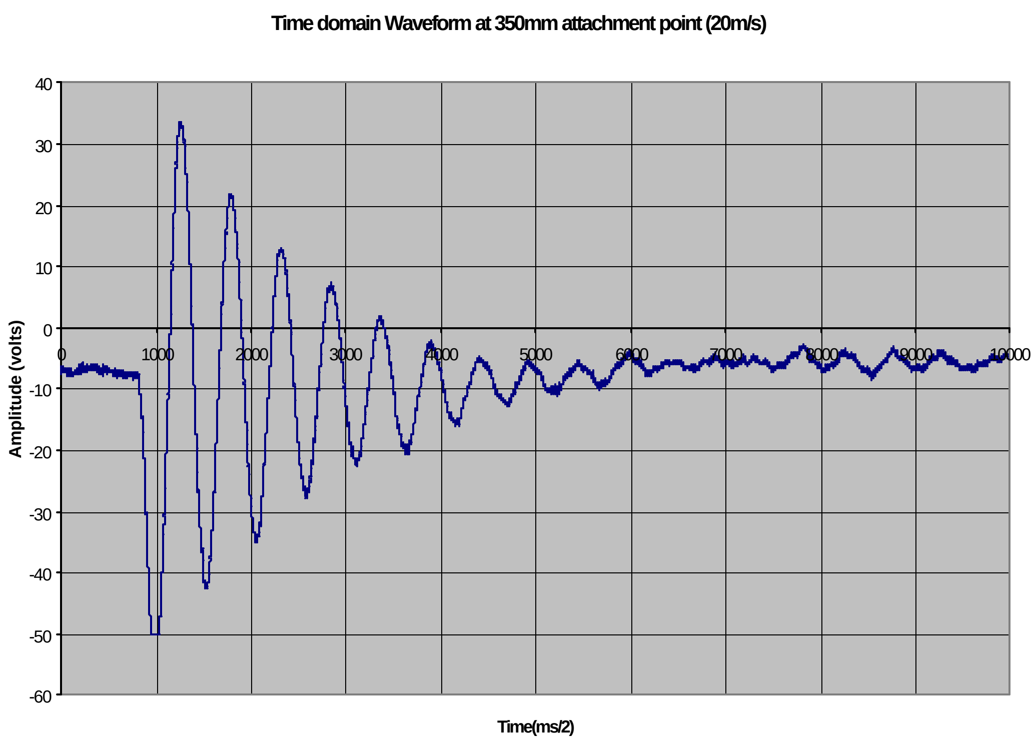

Figure 30. Impulse Response at 20 m/s

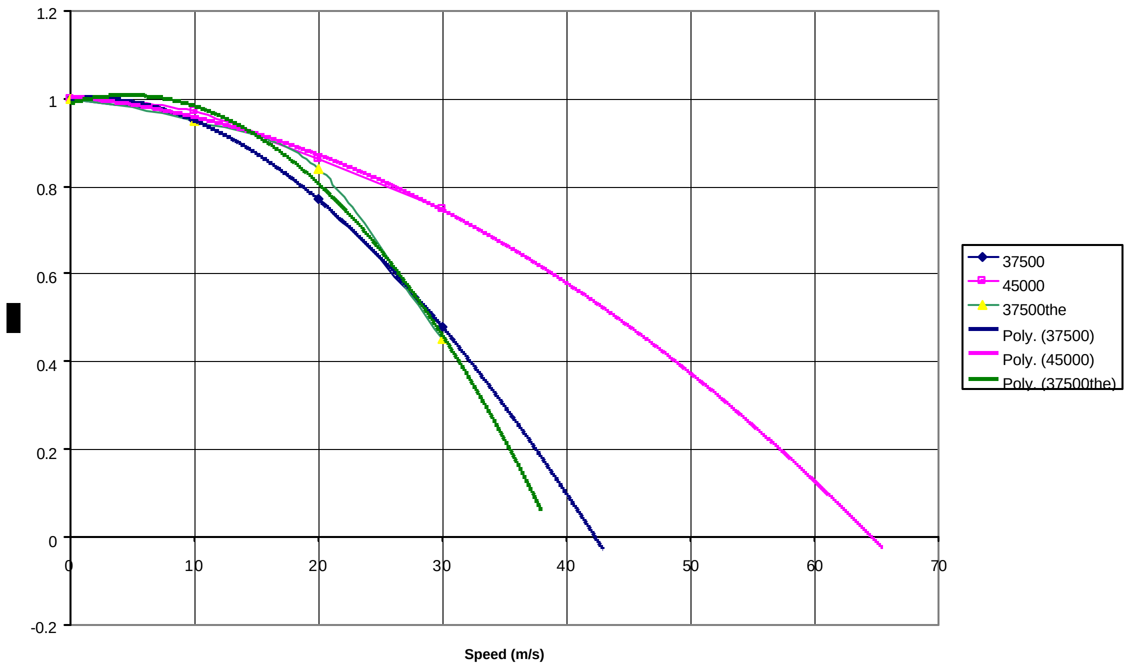

Figure 31. Inverse of Efficiency for Different Spring Stiffnesses

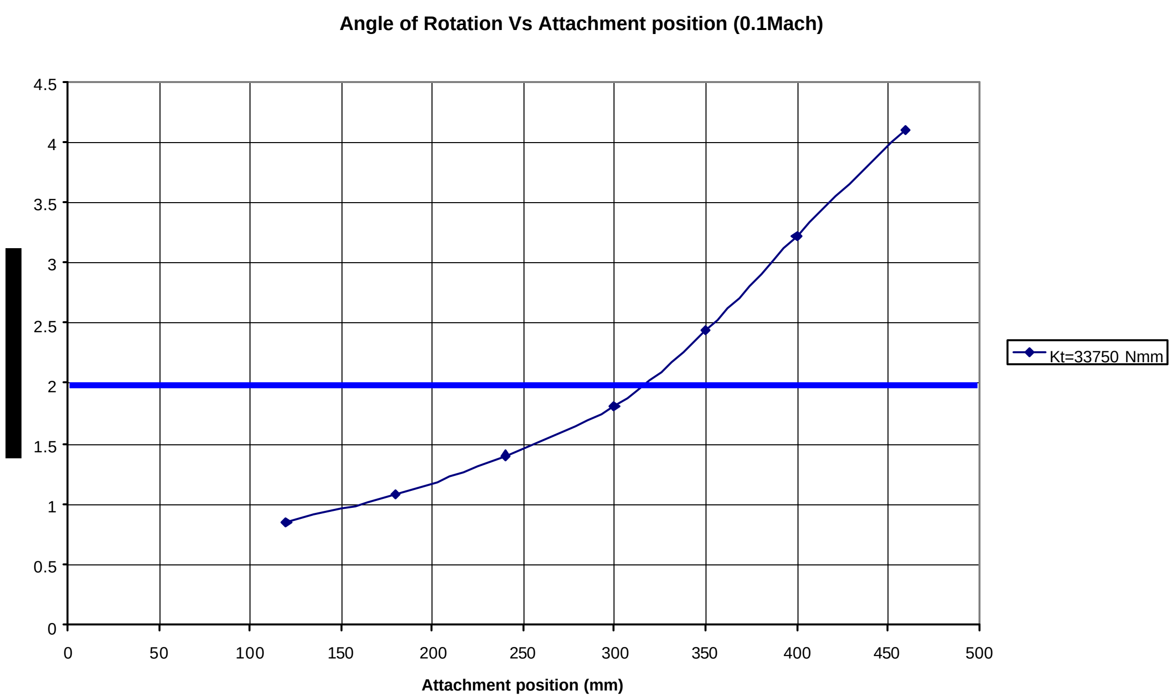

Figure 32. Angle of Rotation vs. Attachment Position - Mach 0.1

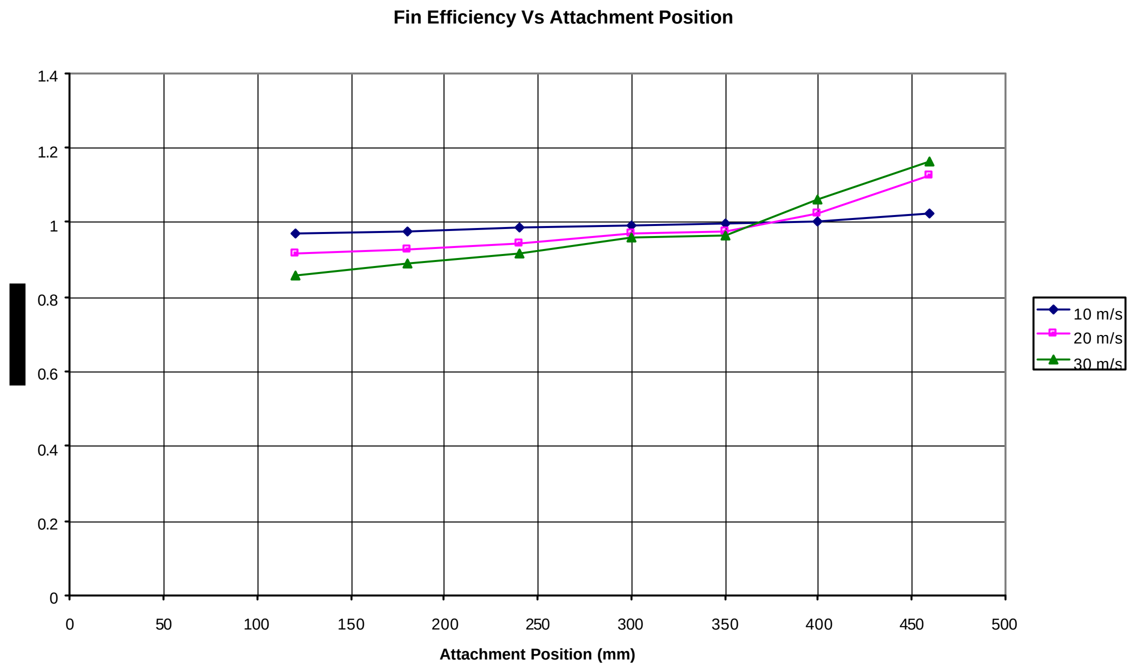

Figure 33. Fin Efficiency vs. Attachment Position 180000Nmm

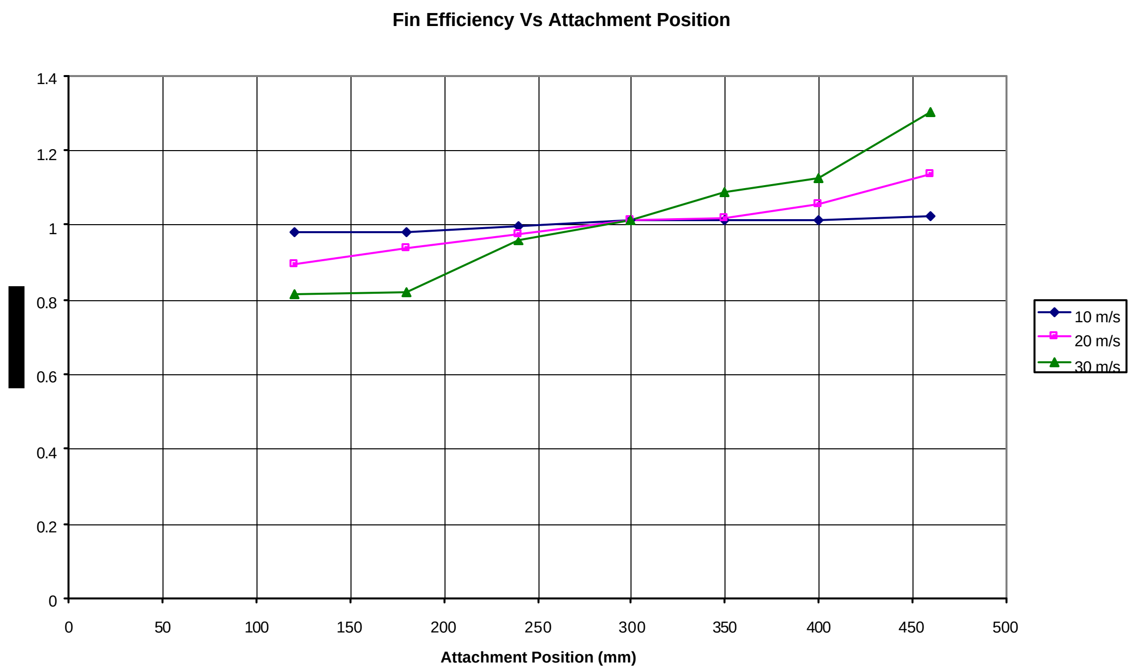

Figure 34. Fin Efficiency vs. Attachment Position 90000Nmm

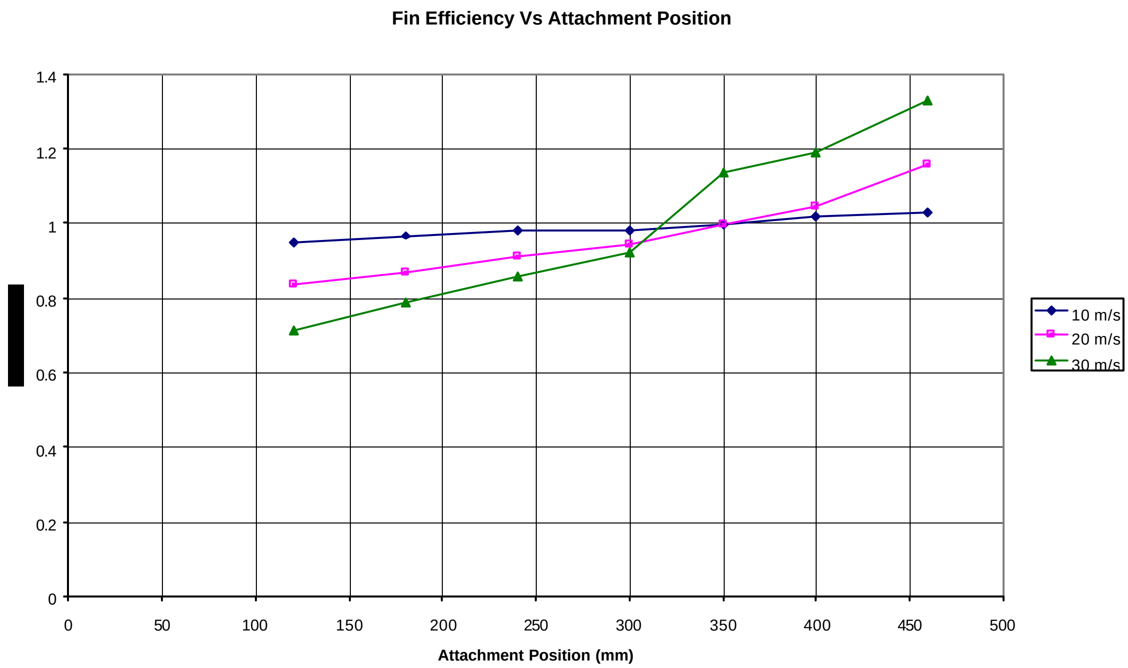

Figure 35. Fin Efficiency vs. Attachment Position 45000Nmm

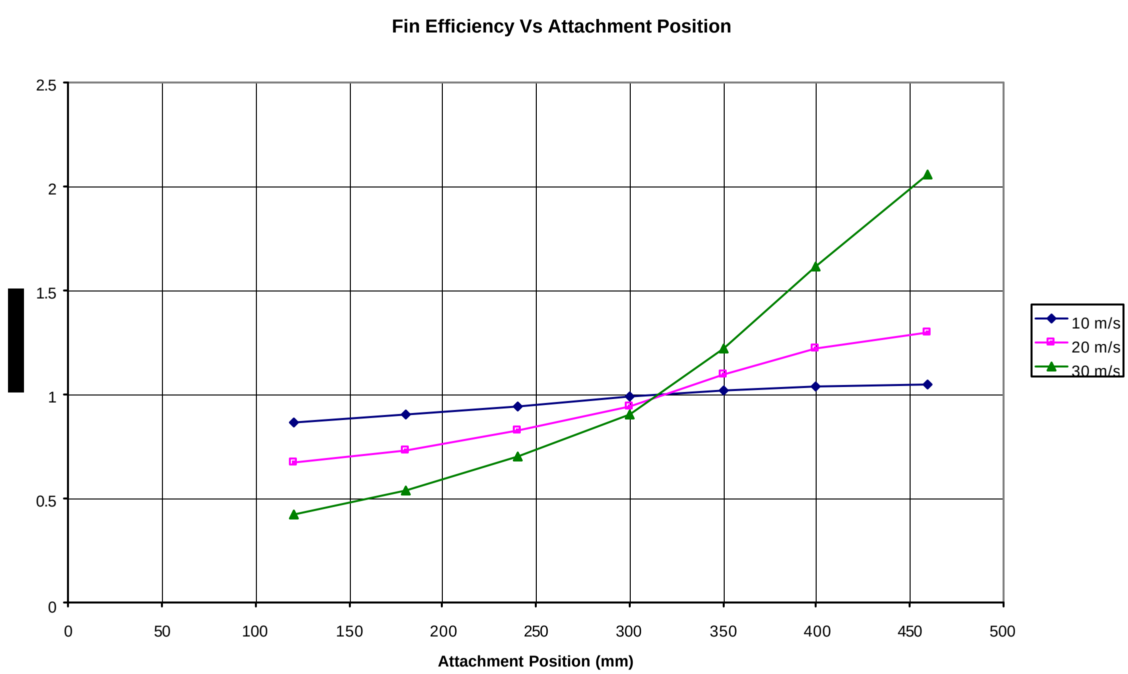

Figure 36. Fin Efficiency vs. Attachment Position 33750 Nmm

Figure 37. Fin Efficiency vs. Attachment Position 180000Nmm 30m/s

.

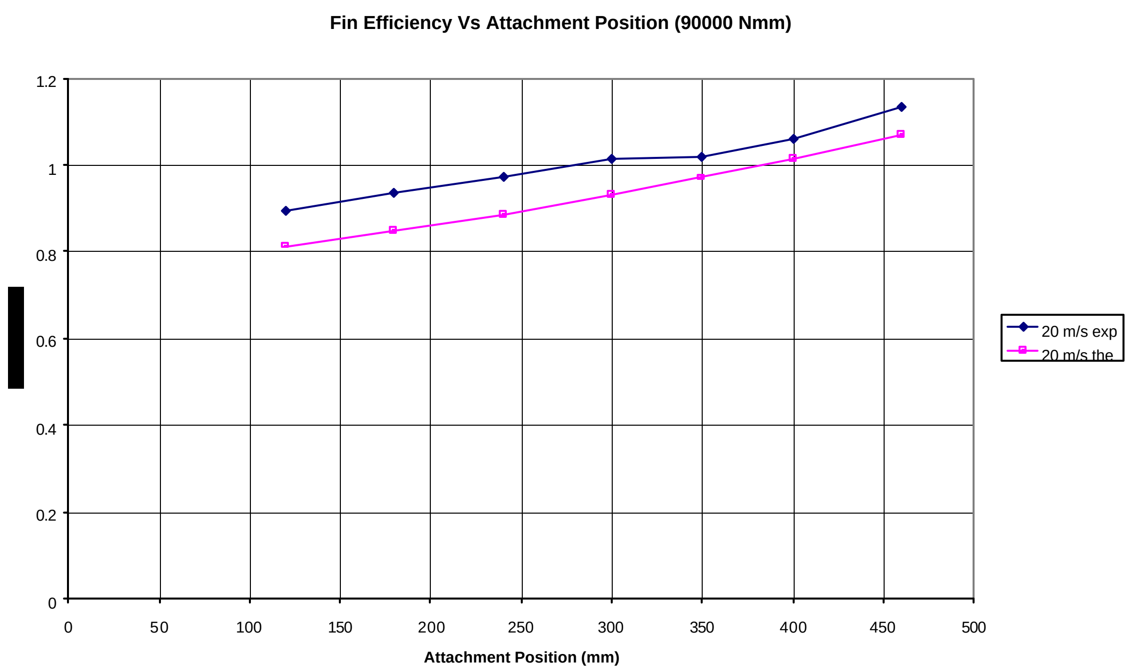

Figure 38. Fin Efficiency vs. Attachment Position 90000Nmm 20m/s

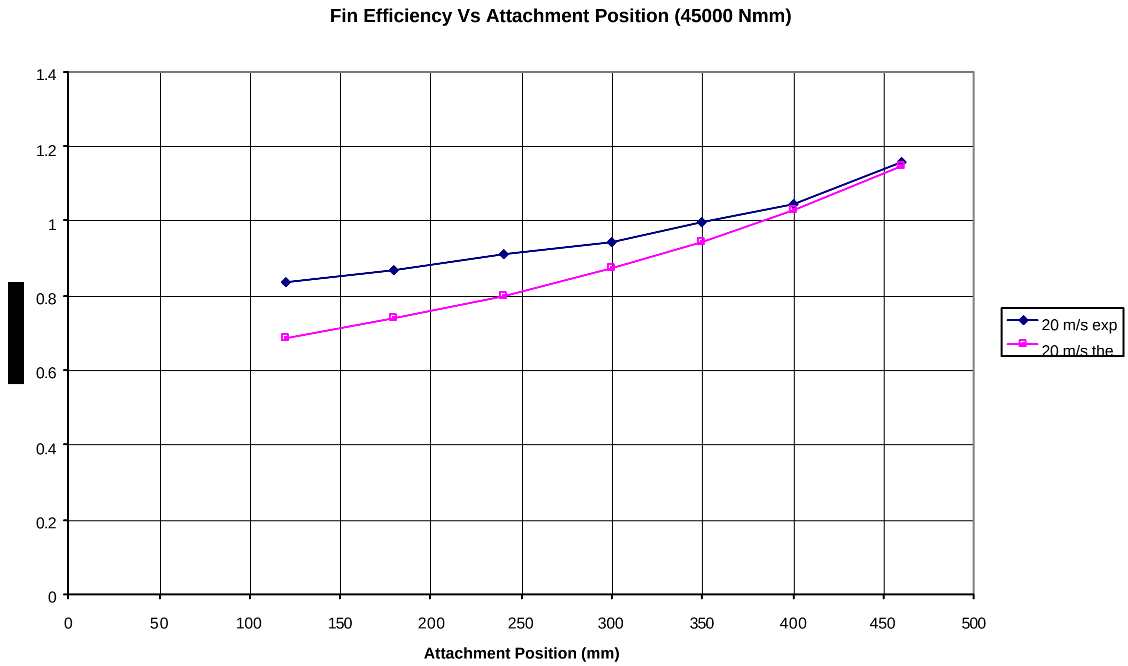

Figure 39. Fin Efficiency vs. Attachment Position 45000 Nmm 20 m/s

Figure 40. Fin Efficiency vs. Attachment Position 33750 Nmm 20m/s

Figure 41. Fin Efficiency vs. Attachment Position 33750 Nmm 30 m/s

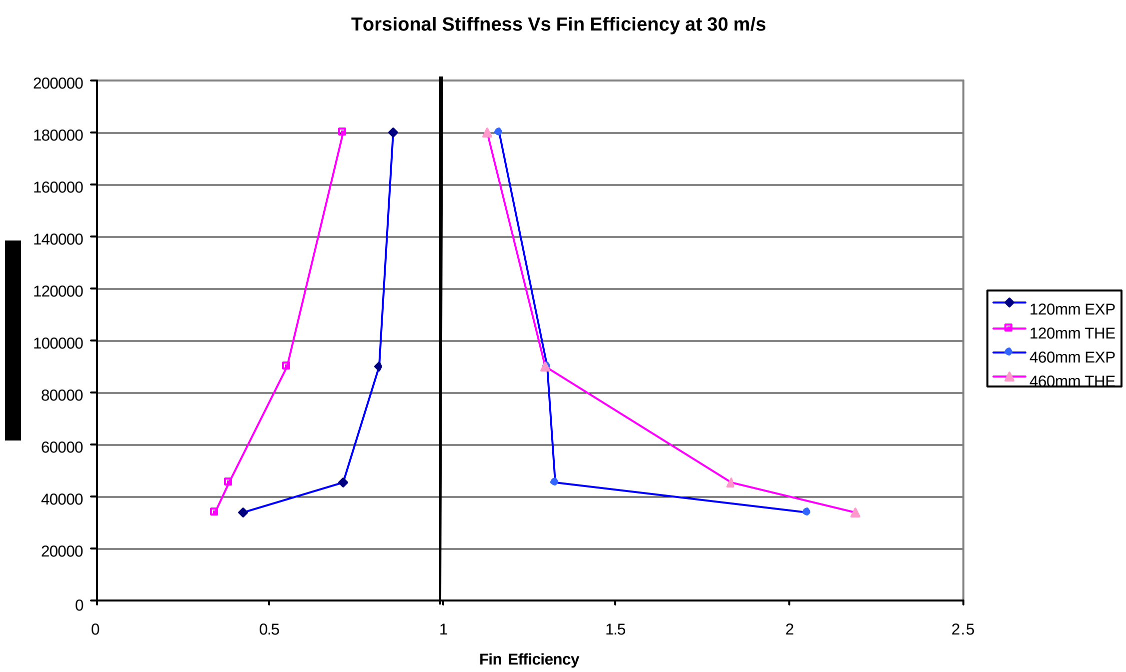

Figure 42. Torsional Stiffness vs Fin Efficiency 30 m/s